Vertical Handoff Decision Algorithms for Providing Optimized Performance in Heterogeneous Wireless Networks

SuKyoung Lee, *Member, IEEE*, Kotikalapudi Sriram, *Fellow, IEEE*, Kyungsoo Kim,
Yoon Hyuk Kim, and Nada Golmie, *Member, IEEE*

Abstract—There are currently a large variety of wireless access networks, including the emerging vehicular ad hoc networks (VANETs). A large variety of applications utilizing these networks will demand features such as real-time, high-availability, and even instantaneous high-bandwidth in some cases. Therefore, it is imperative for network service providers to make the best possible use of the combined resources of available heterogeneous networks (wireless area networks (WLANs), Universal Mobile Telecommunications Systems, VANETs, Worldwide Interoperability for Microwave Access (WiMAX), etc.) for connection support. When connections need to migrate between heterogeneous networks for performance and high-availability reasons, seamless vertical handoff (VHO) is a necessary first step. In the near future, vehicular and other mobile applications will be expected to have seamless VHO between heterogeneous access networks. With regard to VHO performance, there is a critical need to develop algorithms for connection management and optimal resource allocation for seamless mobility. In this paper, we develop a VHO decision algorithm that enables a wireless access network to not only balance the overall load among all attachment points (e.g., base stations and access points) but also maximize the collective battery lifetime of mobile nodes (MNs). In addition, when ad hoc mode is applied to 3/4G wireless data networks, VANETs, and IEEE 802.11 WLANs for a more seamless integration of heterogeneous wireless networks, we devise a route-selection algorithm for forwarding data packets to the most appropriate attachment point to maximize collective battery lifetime and maintain load balancing. Results based on a detailed performance evaluation study are also presented here to demonstrate the efficacy of the proposed algorithms.

Index Terms—High availability, intersystem handover, load balancing, mobility management, quality-of-service (QoS) management, seamless mobility, simulation modeling, vehicular ad hoc network (VANET), vertical handoff (VHO), wireless local area network (WLAN), Worldwide Interoperability for Microwave Access (WiMAX).

I. INTRODUCTION

CONNECTION handoff is no longer limited to migration between two subnets in a wireless local area network (WLAN) or between two cells in a cellular network (generally known as "horizontal handoff"). In addition to roaming and horizontal handoff within homogeneous subnets (e.g., consisting of only IEEE 802.11 WLANs or only cellular networks), supporting service continuity and quality of service (QoS) requires seamless vertical handoffs (VHOs) between heterogeneous wireless access networks. In general, heterogeneous networks can be combinations of many different kinds of networks, e.g., vehicular ad hoc networks (VANETs), WLANs, Universal Mobile Telecommunications Systems (UMTSs), CDMA2000 (code-division multiple access), and mobile ad hoc networks (MANETs). Many new architectures or schemes have recently been proposed for seamless integration of various wireless networks. However, the integration of WLANs and cellular networks has attracted the most attention, because, currently, WLANs and cellular networks coexist and many cellular devices have dual radio-frequency (RF) interfaces for WLANs and cellular access. With regard to VHO performance, there is a critical need for developing algorithms for connection management and optimal resource allocation for seamless mobility. In this paper, we focus on developing such algorithms based on suitable optimization criteria. Since WLAN and cellular access technologies are commonly available and complementary, we focus on these technologies in this paper, but our algorithms are widely applicable across any set of access technologies and applications.

Several interworking mechanisms for combining WLANs and cellular data networks into integrated wireless data environments have been proposed in [1]–[4]. Two main architectures for interworking between IEEE 802.11 WLAN and 3G cellular systems [2]–[4] have been proposed: 1) tight coupling and 2) loose coupling (see Fig. 1). When the loose coupling scheme is used, the WLAN is deployed as an access network complementary to the 3G cellular network. In this approach, the WLAN bypasses the core cellular networks, and data traffic is more efficiently routed to and from the Internet, without having to go over the cellular networks, which could be a potential bottleneck. However, this approach mandates the provisioning

S. Lee is with the Department of Computer Science, Yonsei University, Seoul 120-749, Korea (e-mail: sklee@cs.yonsei.ac.kr).

K. Sriram and N. Golmie are with the Advanced Networking Technologies Division, National Institute of Standards and Technology, Gaithersburg, MD 20878 USA (e-mail: ksriram@nist.gov; ksriram25@gmail.com).

K. Kim is with the Department of Mathematics, Kyonggi University, Suwon 442-760, Korea.

Y. H. Kim is with the Department of Mechanical Engineering, Kyung Hee University, Yongin 446-701, Korea.

Color versions of one or more of the figures in this paper are available online at http://ieeexplore.ieee.org.

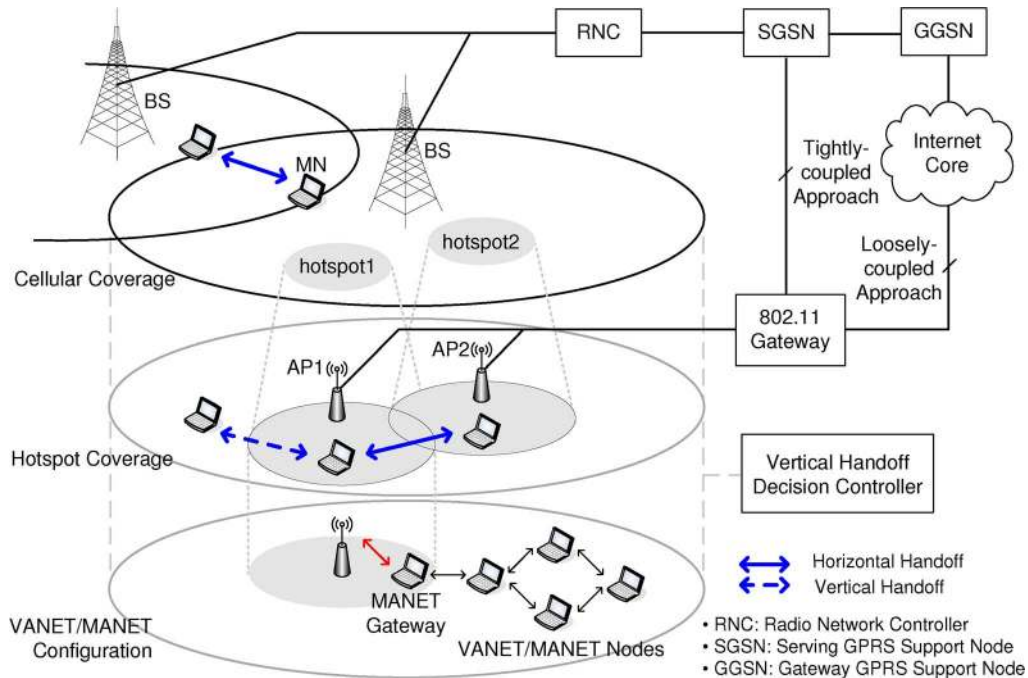Digital Object Identifier 10.1109/TVT.2008.925301

Fig. 1.   Architecture of an integrated heterogeneous network consisting of a WLAN, cellular network, and VANET/MANET.

of special authentication, authorization, and accounting (AAA) servers on the cellular operator for interworking with WLANs' AAA services. On the other hand, when the tight coupling scheme is used, the WLAN is connected to the cellular core network in the same manner as any other 3G radio access network so that the mechanisms for the mobility, QoS, and security of the 3G core network such as UMTS can be reused. As a result, a more seamless handoff between cellular and WLAN networks can be expected in the tightly coupled case, compared to that in the loosely coupled case.

There have also been some research efforts to connect a mobile device equipped with multiple RF interfaces to the most optimal network among a set of available heterogeneous access networks. Vertical mobility is achieved by switching the interface of the mobile device to connect to an alternative target network.

McNair and Zhu [6] introduced important performance criteria to evaluate seamless vertical mobility, e.g., network latency, congestion, battery power, service type, etc. In [7], Guo *et al.* proposed an end-to-end mobility management system that reduces unnecessary handoff and ping-pong effects by using measurements on the conditions of different networks. In [8], various network-layer-based internetwork handover techniques have been addressed, and their performances are evaluated in a realistic heterogeneous network testbed. Nasser *et al.* [9] proposed a VHO decision (VHD) method that simply estimates the service quality for available networks and selects the network with the best quality. However, there still lie ahead many challenges in integrating cellular networks and WLANs (or any combination of heterogeneous networks in general). As pointed out in [5], [6], and [9], known VHO algorithms are not adequate in coordinating the QoS of many individual mobile users or adapting to newly emerging performance requirements for handoff and changing network status. Furthermore, under the current WLAN technology, each mobile device selects

an access point (AP) for which the received signal strength (RSS) is maximum, irrespective of the neighboring network status. Although the attachment to the closest AP is known to consume the least power for the individual mobile device at a given instant, in a situation where many mobile devices try to hand off to the same AP, there would be, in effect, significantly more power consumption at the mobile devices collectively due to increased congestion delays at the AP. In this paper, we tackle the following problem: Given a network of base stations (BSs), APs, and mobile nodes (MNs), and given that an MN is currently experiencing weak or degrading RSS from its current attachment point (BS or AP), how do we find an appropriate attachment point for the MN to connect to (via vertical or horizontal handoff) while optimizing a well-defined objective function? Our objective function includes consideration of the battery life of MNs and load balancing across attachment points. For seamless integration of WLAN and 3/4G wireless networks, we propose a VHD algorithm that not only maximizes the overall battery lifetime of MNs in the same coverage area but also seeks to equitably distribute the traffic load across available APs and BSs. We suggest that this proposed algorithm be implemented in multiple VHD controllers (VHDCs). These VHDCs are located in the access networks and can provide the VHD function for a region covering one or multiple APs and/or BSs. We envision that the decision inputs for the VHDCs will be obtainable via the media-independent handover function (MIHF), which is being defined in IEEE 802.21 [10]. Moreover, when ad hoc mode is applied to 3/4G wireless data networks, VANETs, and IEEE 802.11 WLANs for more seamless integration of heterogeneous wireless networks (see Fig. 1), we devise a route selection algorithm for forwarding data packets to the most appropriate AP/BS to maximize the same objective function, as previously stated. Results based on a detailed performance evaluation study are also presented here to demonstrate the efficacy of
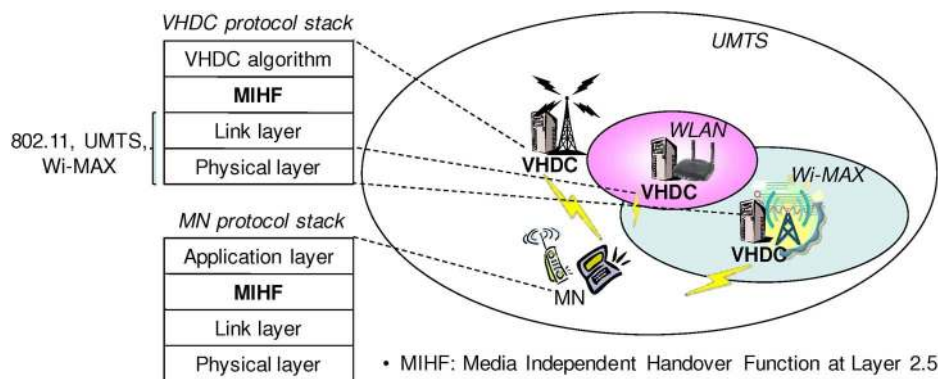
Fig. 2.   VHDC implementation based on IEEE 802.21 MIHF.

the proposed algorithms. It may be mentioned here that route-selection algorithms have previously been studied in the context of WLANs or cellular networks separately [11], [12].

The rest of this paper is organized as follows: We first describe our heterogeneous wireless networking system model and the high-level procedure, followed by the VHDC in Section II. Then, in Section III, we describe the details of optimization algorithms to select an appropriate attachment point. In Section IV, we present a route-selection algorithm in heterogeneous wireless networks that include an ad hoc network (such as a VANET or a MANET) while taking into account the amount of traffic to be forwarded and the load at the attachment points in the route. In Section V, extensive simulation results are presented, and the performance of the proposed algorithms is discussed. Finally, conclusions are stated in Section VI.

II. VHD SYSTEM DESCRIPTION

As shown in Fig. 2, an MN can be existing at a given time in the coverage area of an UMTS alone. However, due to mobility, it can move into the regions covered by more than one access network, i.e., simultaneously within the coverage areas of, for example, an UMTS BS and an IEEE 802.11 AP. Multiple IEEE 802.11 WLAN coverage areas are usually contained within an UMTS coverage area. A Worldwide Interoperability for Microwave Access (WiMAX) coverage area can overlap with WLAN and/or UMTS coverage areas. In dense urban areas, even the coverage areas of multiple UMTS BSs can overlap. Thus, at any given time, the choice of an appropriate attachment point (BS or AP) for each MN needs to be made, and with VHO capability, the service continuity and QoS experience of the MN can significantly be enhanced. A single operator or multiple operators may operate the BSs and APs within a coverage area. Thus, multiple access technologies and multiple operators are typically involved in VHDs. Hence, there is a need for a common language in which the link-layer information and the MNs' battery power information can be exchanged between different networks and/or operators. As described here, this common language is provided by the MIHF of IEEE 802.21.

We also show in Fig. 2 how we envision the VHD to be implemented. We suggest that our proposed VHD algorithm (described in detail in Section III) be implemented in multiple VHDCs. These VHDCs are located in the access networks, as shown in Fig. 2, and can provide the VHD function for a region

covering one or multiple APs and/or BSs. We envision that the decision inputs for the VHDCs will be obtainable via the MIHF, which is being defined in IEEE 802.21 [10]. The VHDC is, conceptually, a network-controlled mobility management entity utilizing the IEEE 802.21 MIHF, and some experimental implementations of this nature are in progress [13], [14]. The MIHF facilitates standards-based message exchanges between the various access networks (or attachment points) to share information about the current link-layer conditions, traffic load, network capacities, etc. The MIHF at an AP also maintains the battery life information of the MNs, which are currently serviced by it.

The goal of our proposed VHDC is to facilitate the optimization of the overall performance of the integrated system of access networks, specifically, in terms of overall battery lifetime and load balancing. Fig. 3 shows the high-level procedure, followed by the VHDC for making VHDs. The algorithmic and mathematical details of this procedure are described in Section III. As shown in Fig. 3, the VHDC obtains link-layer triggers (LLTs) via MIHF [15], [16]. An LLT regarding an MN typically indicates one of these two possibilities: 1) While in service at an AP, the RSS for the MN has dropped below a specified threshold. 2) While in service at a BS, the RSS from one or more APs has just exceeded a specified threshold. In general, if an MN's connection can be supported by an available BS and an available AP, then the AP would be the preferred attachment point for that MN. This is due to the higher data rate and lower bandwidth cost associated with an AP, compared to those associated with a BS. If the LLT indicates possibility 1, then the VHDC tries to search for other networks for connection handoff. In the case that there exist multiple choices of APs for handoff, the VHDC evaluates the APs and then directs a handoff operation to the network with optimal performance/cost. On the other hand, if no other APs are found for a possible handoff, then the cellular network would then be considered the best available wireless network. If the LLT indicates possibility 2, then the MN would be a candidate for VHO from a BS (UMTS or WiMAX) to an AP (WLAN). As described before, the performance/cost can be in the form of the collective battery lifetime of the MNs and/or load balancing across the APs/BSs. We can choose a performance metric that is tunable with weighing parameters α and β and could be tuned to represent only longevity of battery lifetime over all MNs or only load balancing across all APs/BSs or a weighted
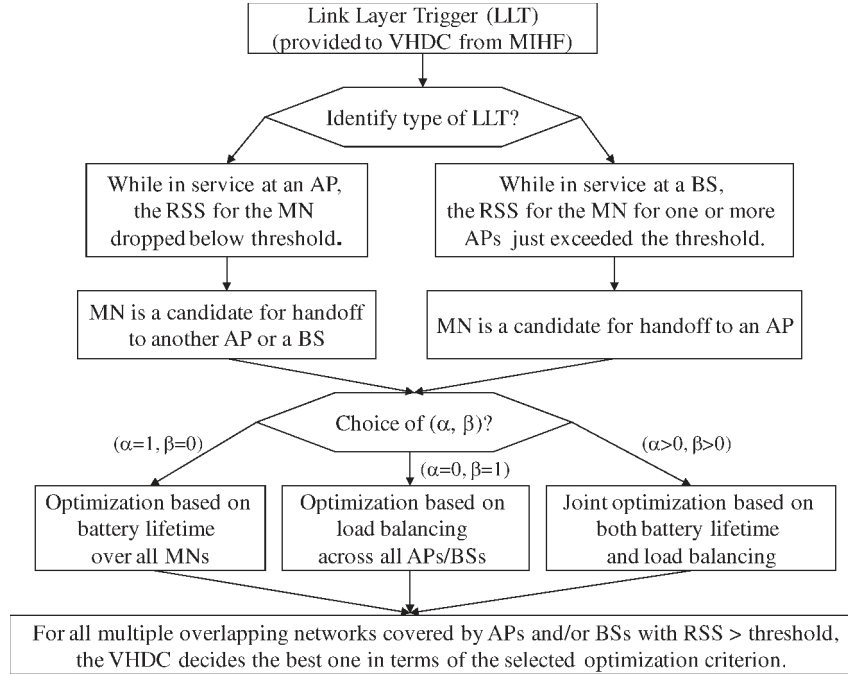
Fig. 3.   Flowchart for the high-level procedure used by the VHDC.

combination of the two. As seen in the last step of the procedure in Fig. 3, irrespective of the current network type, the VHDC decides the best network among multiple overlapping networks (covered by APs or BSs), based on a selected optimization criterion. The details of this last step follow in the next section.

III. VERTICAL HANDOVER DECISION ALGORITHM TO OPTIMIZE THE SYSTEM PERFORMANCE

In this section, details of the optimization techniques used in our VHD algorithm and implemented in the VHDC are provided. The WLAN hotspots are typically configured as small cells within the aforementioned "cellular coverage area" of GPRS/UMTS or CDMA2000, which is relatively larger compared with WLAN hotspots, as shown in Fig. 1. Since many variables are used in this paper, a glossary of variable names and definitions is provided in Table I.

Let $A = \{a_1, \ldots, a_N\}$ and $C = \{c_1, \ldots, c_M\}$ be the sets of APs in a cellular coverage area and BSs covering the cellular coverage area, respectively. Note that, usually, $M = 1$, except in the case of a highly dense urban deployment. Even when $M > 1$, M is much smaller than N, because, typically, many APs are deployed within a cellular coverage area. The VHDC maintains the sets A and C covering the cellular coverage area as a list of candidate attachment points. It adds all available WLAN APs into set A and collects the information about load status on every AP in set A and every BS in set C. Note that, in this section, we take into account only $a_i \in A (1 \leq i \leq N)$ and $c_{\hat{i}} \in C (1 \leq \hat{i} \leq M)$ as candidate attachment points, whereas, in the next section, each MN in ad hoc networking mode would also be considered as a possible attachment point. In the cellular coverage area, $\bar{U} = \{u_1, \ldots, u_K\}$ is defined as the set of all MNs. Each MN is either requesting a handoff (or just turned on) or is currently serviced by an AP ($\in A$) or BS ($\in C$), with no need for mobility at the time of optimization decision. Thus,

set $\bar{U}$ can be divided into the following two subsets at a certain time t:

$$U_t = \{u_{n_1}, u_{n_2}, \ldots, u_{n_{m(t)}}\}$$

where $m(t)$ is the number of MNs requesting handoff at time t, and $n_1, \ldots, n_{m(t)}$ are the corresponding indexes of those MNs, and

$$V_t = \bar{U} - U_t$$

which represents the set of MNs that have a good connection (i.e., not requiring handoff) to an AP or a BS.

Each AP a_i and each BS $c_{\hat{i}}$ are assumed to have maximum bandwidths of B_i and $B_{\hat{i}}^{(c)}$, respectively. Let $\hat{i}$ denote $i - N$ ($N + 1 \leq i \leq N + M$). Let $w(i)$ ($1 \leq i \leq N + M$) denote the predefined costs or weights for the bandwidths of AP a_i ($1 \leq i \leq N$) and BS $c_{\hat{i}}$ ($N + 1 \leq i \leq N + M$). For simplicity, we define two different weights, depending on whether the wireless access network is a WLAN or a cellular network. That is, for APs $a_i \in A$ ($1 \leq i \leq N$), $w(i) = w_a$, and for BSs $c_{\hat{i}}$ ($1 \leq \hat{i} \leq M$), $w(i) = w_c$. Each $a_i \in A$ has a limited transmission range and serves only users that reside in its range. Set V_t is divided into subsets $V_t^{(a)}$ and $V_t^{(c)}$, depending on whether $u_j \in V_t$ has a connection in a WLAN or a cellular network, respectively. Note that the $|U_t|$ MNs that are candidates for VHO can belong in a WLAN or a cellular network, subsequent to the handoff decision.

For IEEE 802.11 products, it is known that an AP is able to maintain the average bit rate information for the MNs that are currently associated with it [17], [18]. Thus, each AP ($a_i \in A$) or BS ($c_{\hat{i}} \in C$) can maintain the effective data rates e_{ij} and $e_{\hat{i}j}^{(c)}$ for MN u_j when it belongs to $V_t^{(a)}$ or $V_t^{(c)}$, respectively. However, for each MN $u_j \in U_t$, the AP to which the MN will hand off is not able to evaluate the effective data rate for the

TABLE I
GLOSSARY OF VARIABLE DEFINITIONS

Variable	Definition
N	Number of APs
M	Number of BSs
$\bar{U}$	Set of all Mobile Node (MNs)
$|\bar{U}|$	Total number of MNs (K)
u_j	MN j ($1 \leq j \leq K$)
r_j	Bandwidth (i.e., data rate) requested by u_j ($1 \leq j \leq K$)
U_t	Set of MNs requesting vertical handoff (VHO) at time t
$|U_t|$	Number of MNs requesting handoff at time t (equals $m(t)$)
V_t	$V_t = \bar{U} - U_t$
$V_t^{(a)}$	Subset of MNs in V_t that have connection in a WLAN at t
$V_t^{(c)}$	Subset of MNs in V_t that have connection in a cellular network at t
	$V_t = V_t^{(a)} + V_t^{(c)}$ or $V = V_a + V_c$ (dropping t)
	$U_t, V_t, V_t^{(a)}, V_t^{(c)} \Rightarrow U, V, V_a, V_c$ (dropping t)
$|V_a|$	Number of MNs that have a connection in a WLAN at time t
$|V_c|$	Number of MNs that have a connection in a a cellular network at time t
$\hat{i}$	$i - N$; $1 \leq \hat{i} \leq M$ corresponds to $N + 1 \leq i \leq N + M$
B_i	Maximum bandwidth which an AP a_i ($1 \leq i \leq N$) can provide
$B_{\hat{i}}^{(c)}$	Maximum bandwidth which a BS $c_{\hat{i}}$ can provide
$w(i)$	Price/weight for WLAN and cellular bandiwdths; w_a ($1 \leq i \leq N$) and w_c ($N + 1 \leq i \leq N + M$)
e_{ij}	Effective bandwidth of MN u_j when it is attached to AP i
$e_{ij}^{(c)}$	Effective bandwidth of MN u_j when it is attached to BS i
ρ_i	Load at AP a_i ($1 \leq i \leq N$); Load at BS c_i ($N + 1 \leq i \leq N + M$)
z_i	Equals B_i for $0 \leq i \leq N$ and $B_{\hat{i}}^{(c)}$ for $N + 1 \leq i \leq N + M$
p_j	Available battery power of MN j
p_{ij}	Power consumption rate per unit time for MN j when attached to AP a_i
$p_{ij}^{(c)}$	Power consumption rate per unit time for MN j when attached to BS c_i
p_j^b	Power consumption amount per byte of transmission at MN j
RSS_{ij}	Received signal strength for MN j from AP a_i or BS c_i
θ_a	RSS threshold to connect to AP
θ_c	RSS threshold to connect to BS

MN due to the absence of active signaling between the AP and the MN when they are not connected. Thus, a requested data rate r_j is defined for each MN $u_j \in U_t$. Otherwise, if we assume that every MN is equipped with client software that periodically collects the bit rate information for every AP/BS in its neighborhood by using beacon messages/pilot bursts, it is possible to evaluate the effective bit rates e_{ij} and $e_{ij}^{(c)}$ from each AP $a_i \in A$ and BS $c_{\hat{i}} \in C$, respectively, to each MN $u_j \in U_t$. The collected information about the effective bit rate is available to the VHDC via the IEEE 802.21 MIHF.

Since our proposed selection algorithms are performed at a certain time instant t, from now on, we shall omit the subscript t from $U_t, V_t, V_t^{(a)}$, and $V_t^{(c)}$ for notational convenience and for clarity of understanding. Thus, U, V, V_a, and V_c will be used instead. Now, we define the load ρ_i on AP a_i or on BS $c_{\hat{i}}$ in a cellular coverage area as follows:

Definition 1: For each AP $a_i \in A$ ($1 \leq i \leq N$), the load on AP a_i is

$$\rho_i = \sum_{u_j \in V_a} e_{ij}, \qquad \text{for } 1 \leq i \leq N \qquad (1)$$

whereas the load on BS $c_{\hat{i}}$ is

$$\rho_i = \sum_{u_j \in V_c} e_{\hat{i}j}^{(c)}, \qquad \text{for } N + 1 \leq i \leq N + M. \qquad (2)$$

The preceding definition of load does not deliberately take into account the calls that are requesting handoff and will move

away from the AP in consideration when the time decision is made. As a matter of fact, it is possible to compute ρ_i ($1 \leq i \leq N + M$), because an AP or BS is able to maintain the bit rate information for all the MNs connected to itself.

Associated with each MN u_j ($1 \leq j \leq K$) is a quantity p_j that denotes the available amount of power or the initial amount of power when it is just attached to a network. Normally, p_j would be at its maximum when the battery is fully charged. Let p_{ij} denote the power consumption per unit of time needed at MN u_j ($1 \leq j \leq K$) to reach an AP a_i ($1 \leq i \leq N$). The value of p_{ij} depends on the number of MNs attached to AP a_i and the data rate requested by MN u_j, that is, the larger the number of power-on nodes attached to the same AP, the more power consumed by each MN, because they each get lower rates and hence need to connect longer. With greater use of applications requiring higher data rate, the MN will consume power at higher rates. Thus, the amount of load at the AP has an impact on the power consumed by MNs as $p_{ij} \propto \rho_i$. Similarly, $p_{\hat{i}j}^{(c)}$ ($\propto \rho_{N+\hat{i}}$) stands for the power level needed at MN u_j to reach BS $c_{\hat{i}}$.

When each MN u_j ($1 \leq j \leq K$) is associated with a certain AP a_i ($1 \leq i \leq N$) or BS $c_{\hat{i}}$ ($1 \leq \hat{i} \leq M$), a formal definition of the battery lifetime matrix for the MNs with respect to each attachment point in the cellular coverage area is given as follows:

Definition 2: Let $\mathbf{L} = \{l_{ij}\}_{(N+M) \times K}$ be the battery lifetime matrix where matrix element l_{ij} ($1 \leq i \leq N + M$) denotes the

battery lifetime of u_j, supposing that MN u_j hands off to AP a_i $(1 \leq i \leq N)$, whereas $l_{(N+\hat{i})j}$ $(1 \leq \hat{i} \leq M)$ is the battery lifetime of u_j in case that MN u_j hands off to BS $c_{\hat{i}}$. Then, for each MN u_j $(1 \leq j \leq K)$, we have

$$l_{ij} = \frac{p_j}{p_{ij}}, \qquad \text{for } 1 \leq i \leq N \qquad (3)$$

$$l_{ij} = \frac{p_j}{p_{ij}^{(c)}}, \qquad \text{for } N+1 \leq i \leq N+M \qquad (4)$$

where it is assumed that every $l_{ij} > 0$ in this study.

The significance of the assumption that $l_{ij} > 0$ is that the MNs never disconnect due to battery outage. Thus, the population of MNs in the system remains constant. In our simulation tests, this is ensured by choosing a sufficient large initial battery power for all MNs. Matrix $\mathbf{L}$ plays a significant role in decisions at the VHDC regarding which attachment point should be selected among sets A and C for the MNs requiring handoff. The different cost functions used in the optimization methods leading to handoff decisions will formally be defined later in this section.

To formulate the optimal VHD problem, a binary variable x_{ij} is defined to have a value of one $(x_{ij} = 1)$ if user u_j is associated with AP a_i $(1 \leq i \leq N)$ or BS $c_{\hat{i}}$ $(N+1 \leq i \leq N+M)$, and zero $(x_{ij} = 0)$ otherwise. Let RSS_{ij} $(1 \leq i \leq N+M)$ be the RSS for MN j from AP a_i or BS $c_{\hat{i}}$. Let θ_a and θ_c denote the RSS thresholds for the MN's connection to AP and BS, respectively. Then, we can define an association matrix $\mathbf{X}$ consisting of x_{ij} as follows:

Definition 3: Let $\mathbf{X} = \{x_{ij}\}_{(N+M) \times K}$ be an association matrix for a cellular coverage area such that

$$\sum_{1 \leq i \leq N+M} x_{ij} = 1, \qquad \text{for } 1 \leq j \leq K \qquad (5)$$

$$x_{ij} \in \{0, 1\} \qquad (6)$$

$$x_{ij} = 0 \text{ if } RSS_{ij} < \begin{cases} \theta_a, & \text{for } 1 \leq i \leq N \\ \theta_c, & \text{for } N+1 \leq i \leq N+M \end{cases} \qquad (7)$$

where x_{ij} $(1 \leq i \leq N, 1 \leq j \leq K)$ and $x_{(N+\hat{i})j}$ $(1 \leq \hat{i} \leq M, 1 \leq j \leq K)$ are binary indicators, each of which has a value of 1 if and only if, for the former, MN u_j hands off to AP a_i, whereas, for the latter, MN u_j hands off to BS $c_{\hat{i}}$. Moreover, let $\mathcal{X}$ be the set of all association matrices.

The BSs collectively provide full coverage for the entire region of interest. The aforementioned Definition 3 accordingly assures that each MN requesting handoff is covered by either a BS or an AP.

Definition 4: The battery lifetime of MN $u_j \in U$ for an association matrix $\mathbf{X} = \{x_{ij}\}$, $lt_j(\mathbf{X})$ is defined as

$$lt_j(\mathbf{X}) = \sum_{1 \leq i \leq N+M} l_{ij} x_{ij}. \qquad (8)$$

We can define the requested data rate on AP a_i and BS $c_{\hat{i}}$ for an arbitrary association matrix as follows:

Definition 5: Let γ_i $(1 \leq i \leq N+M)$ denote the total requested data rate on AP a_i $(1 \leq i \leq N)$ and BS $c_{\hat{i}}$ $(1 \leq \hat{i} \leq M)$. Let r_j denote the data rate requested by MN u_j $(1 \leq j \leq K)$. Then, for any $\mathbf{X} = \{x_{ij}\} \in \mathcal{X}$

$$\gamma_i(\mathbf{X}) = \sum_{u_j \in U} r_j x_{ij}. \qquad (9)$$

In case that each MN $u_j \in U$ is able to evaluate the effective bit rates e_{ij} and $e_{ij}^{(c)}$ from the candidate APs (i.e., those with $RSS_{ij} > \theta_a$) and the candidate BSs (i.e., those with $RSS_{ij} > \theta_c$), (9) in Definition 5 is replaced by

$$\gamma_i(\mathbf{X}) = \begin{cases} \sum_{u_j \in U} e_{ij} x_{ij}, & \text{for } 1 \leq i \leq N \\ \sum_{u_j \in U} e_{ij}^{(c)} x_{ij}, & \text{for } N+1 \leq i \leq N+M. \end{cases} \qquad (10)$$

For the given battery lifetime matrix $\mathbf{L}$, we formulate the VHD problem to maximize the battery lifetime (network wide) as follows:

$$\mathbf{Max}\text{-}L : \text{Max}_{\forall \mathbf{X} \in \mathcal{X}} \sum_{u_j \in U} lt_j(\mathbf{X}) \qquad (11)$$

subject to

$$\rho_i + \gamma_i(\mathbf{X}) \leq \begin{cases} B_i, & \text{for } 1 \leq i \leq N \\ B_{\hat{i}}^{(c)}, & \text{for } N+1 \leq i \leq N+M \end{cases} \qquad (12)$$

where the constraint in (12) ensures that the total load on each attachment point cannot exceed the maximum bandwidth supported by each AP or BS. With regard to (11), it may be noted that the battery lifetimes of $u_j \in V$, where $V = V_a \cup V_c$, do not play a role in the optimization (at each decision epoch). However, all MNs are included for reporting the average remaining battery lifetime in the course of our simulations (Section V).

In the problem formulation of **Max**-L in (11), the total battery lifetime of the system is maximized, without considering fairness with regard to the individual battery lifetime of different MNs. Thus, the max-min fairness is taken into account as follows:

$$\mathbf{Max/Min}\text{-}L : \text{Max}_{\forall \mathbf{X} \in \mathcal{X}} \left(\text{Min}_{1 \leq j \leq K} lt_j(\mathbf{X}) \right) \qquad (13)$$

subject to the same constraint as stated for **Max**-L in (12). While the earlier formulation of **Max**-L in (11) increases the total battery lifetime, it may, in some situations, compromise the MNs with already lower remaining power. Thus, we mention this alternative **Max/Min-L** formulation, but in this paper, our focus is more toward joint optimization of battery lifetime and fairness in terms of the distributedness of load at the APs/BSs.

We now turn to the problem of distributing the overall load in a cellular coverage area. Lemma 1 in the Appendix captures the fact that minimizing the sum of squared numbers is equivalent to minimizing the standard deviation of the numbers when the mean is constant. Since the standard deviation represents the degree of variation, we aim for the load per AP or BS in
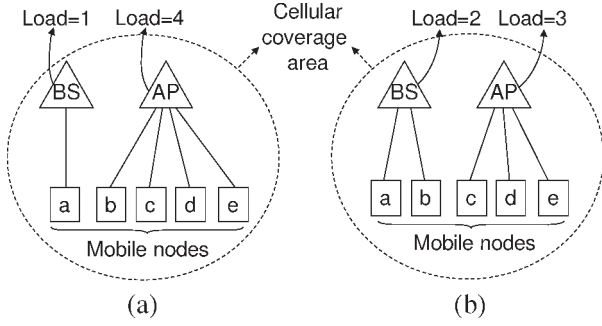
Fig. 4. Examples of achieved load distribution across attachment points when **Opt**-F is applied. (a) Case 1. (b) Case 2.

the cellular coverage area to stabilize around a mean value M with small deviations.

Property 1: The total load from all the MNs of U $\sum_{1 \leq i \leq N+M} \gamma_i(\mathbf{X})$ does not change, irrespective of what values $\mathbf{X}$ has. Thus, in a cellular coverage area, the expression $1/(N+M) \sum_{1 \leq i \leq N+M} w(i)((\rho_i + \gamma_i(\mathbf{X}))/z_i)$ also becomes invariant to the decision (i.e., $\mathbf{X}$) at the time of performing the optimization algorithm, where z_i is a maximal load that each AP or BS can tolerate.

In Property 1, $z_i = B_i$ for $1 \leq i \leq N$, and/or $z_i = B_{\hat{i}}^{(c)}$ for $N + 1 \leq i \leq N + M$ [as in (12)], noting that $\hat{i} = i - N$.

Based on Lemma 1 (in the Appendix) and Property 1, we define a load-based cost function F and formulate the following optimization for the distributedness of the load:

$$\mathbf{Opt}\text{-}F : \text{Min } F = \text{Min}_{\forall \mathbf{X} \in \mathcal{X}} \sum_{1 \leq i \leq N+M} w(i) \left(\frac{\rho_i + \gamma_i(\mathbf{X})}{z_i} \right)^p \tag{14}$$

subject to

$$\rho_i + \gamma_i(\mathbf{X}) \leq z_i, \qquad \text{for } 1 \leq i \leq N + M \tag{15}$$

where $p = 2$ is recommended (see the following discussion). Minimizing the cost function in (14) results in preventing the BSs and APs with already higher load from being more congested.

Fig. 4(a) and (b) shows and compares two cases of the achieved load distributions using (14). In this example, $K = 5$, $M = 1$, and $N = 1$. Consider a cellular coverage area with two attachment points and five mobile users named "a" to "e", where it is assumed that the weights of each MN for the cellular network and WLAN are the same (i.e., $w_c = w_a$) and that the maximum available bandwidth at an AP or a BS is 5 (i.e., $z_1 = z_2 = 5$) for simplicity. Assume that the data rate to every MN is 1. When $p = 1$, the attachment point selection may result in Fig. 4(a) or Fig. 4(b), because $(1/5) + (4/5)(= 1) = (2/5) + (3/5)(= 1)$, that is, when $p = 1$, there is no difference between the two cases in Fig. 4(a) and (b), because the total loads in the two cases are the same. However, when $p = 2$, the attachment points are selected as in Fig. 4(b), because $(1/5)^2 + (4/5)^2(= 0.68) > (2/5)^2 + (3/5)^2(= 0.52)$ based on (14). Thus, the cost function in (14) with $p = 2$ provides fairness from the load-balancing point of view when deciding an attachment point for an MN that requires handoff. This, in turn, results in an

improvement in the overall QoS (i.e., lower delays and packet losses) at the attachment points.

To accomplish a joint optimization of the total battery lifetime and the fairness of load in a cellular coverage area, we formulate a combined cost function with parameters α and β as follows:

$$G(\mathbf{X}, \alpha, \beta) = \alpha \sum_{u_j \in U} lt_j(\mathbf{X}) - \beta \sum_{1 \leq i \leq N+M} w(i) \left(\frac{\rho_i + \gamma_i(\mathbf{X})}{z_i} \right)^2 . \tag{16}$$

Minimizing the cost function in (14) is equivalent to maximizing the negative of the same cost function, because $(\rho_i + \gamma_i(\mathbf{X}))/z_i < 1$. Thus, we have the joint optimization statement of the total battery lifetime and the fairness of the load as follows:

$$\mathbf{Opt}\text{-}G : \text{Max } G(\mathbf{X}, \alpha, \beta) \tag{17}$$

with the constraints of (15). In (17), when $\alpha = 1$ and $\beta = 0$, it is evident that (17) is an equivalent optimization problem of (11). Furthermore, the optimization problem $\text{Max}_{\forall \mathbf{X} \in \mathcal{X}} G(\mathbf{X}, 0, 1)$ subjected to the constraint in (15) is equivalent to **Opt**-F.

IV. OPTIMIZATION OF BATTERY LIFETIME IN HETEROGENEOUS NETWORKS INCLUDING AD HOC MODE

A. Integrated WLAN and Cellular Networking System Including Ad Hoc Networking Mode

We now consider network architectures where, in addition to cellular networks and WLANs, peer-to-peer communications is further enabled using the IEEE 802.11 ad hoc mode [11], [12] (see also Fig. 1). Now see seek to generalize the algorithm to select the most appropriate attachment point by considering the further selection of intermediate MNs to relay data packets to that attachment point.

In this system with ad hoc networking, cooperating MNs form a MANET/VANET using the IEEE 802.11 interface in an ad hoc mode. When an MN that is actively receiving data frames from a BS of the cellular network or an AP experiences a low downlink channel rate and the VHDC cannot find an alternative direct attachment point (i.e., BS or AP) for the MN, a route will be selected via the MANET/VANET to allow the MN to access an appropriate attachment point.

The dynamic source routing (DSR) technique [19], [20] is used with suitable modification as the underlying route discovery protocol in our system. As shown in Fig. 5, the MN (i.e., source labeled as *src*) sends out a *route request* message using its IEEE 802.11 interface. This *route request* message is broadcast through the ad hoc network according to the route discovery protocol. The objective is to find an optimal relay route in terms of overall battery lifetime, to reach a node (i.e., proxy node) with a high downlink channel rate to an attachment point. To prevent the *route request* message from being sent to all the APs and the BS in a cellular coverage area, the number of hops is limited by using the time-to-live (TTL) field in the *route request*. Thus, the spread of a *route request* is controlled
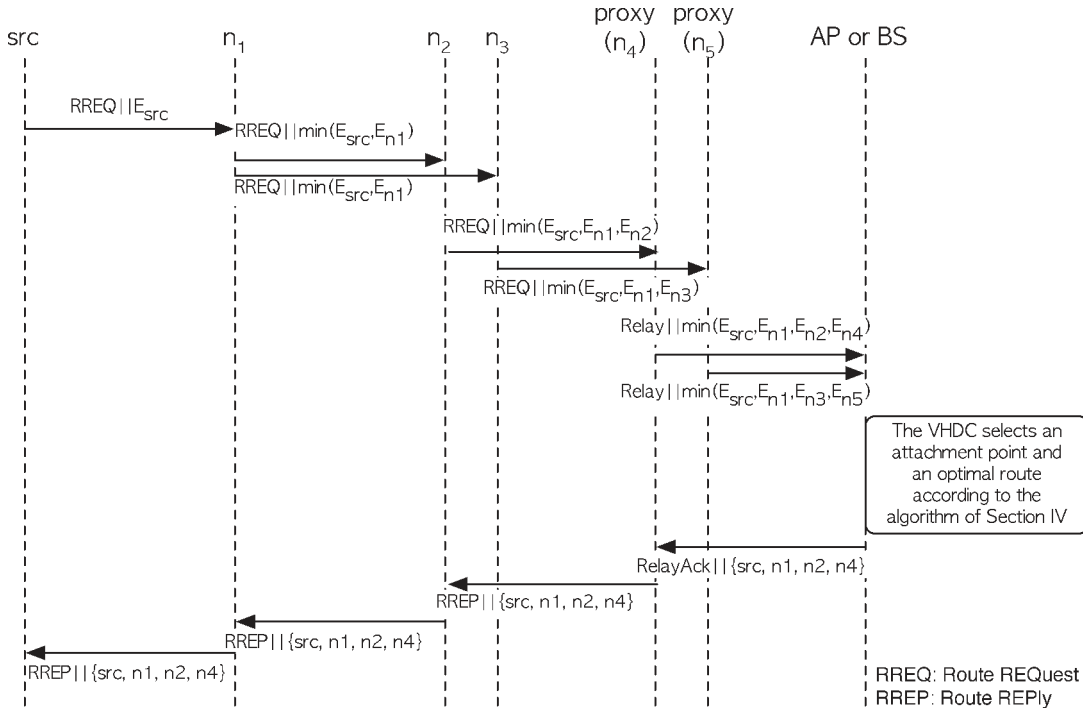
Fig. 5. Example procedure for discovering a relay route to a proxy node, where a relay route {source, node n_1, node n_2, proxy node n_4} is selected.

only to nearby attachment points located within a predesignated number of hops over the ad hoc network.

Again referring to Fig. 5, the candidate proxy node sends a *relay* message to its BS or AP. Once the BS or AP receives the *relay* message, the VHDC (in Section II) selects an attachment point and the best route to the attachment point based on the algorithm that is presented in Section IV-B. The selected attachment point updates its routing table entry for the MN while sending a *relay ack* message to the proxy node. Then, the proxy node returns a *route reply* to the MN that initiated the *route request*. When the proxy node receives a data frame from the BS or AP, it forwards the frame to the next relay node. This forwarding process continues via the IEEE 802.11 interfaces of all the relay nodes on the selected route until the MN receives the frame. For the case when the downlink channel rate of the proxy node goes below a certain level due to its mobility, DSR is modified for the proxy node to piggyback its degraded downlink channel rate in data frames that are forwarded to the source MN so that it could begin another round of route discovery to find another optimal relay route.

We will now proceed to presenting the details of the algorithm for the selection of the relay and proxy nodes that constitute the source MN's route toward a BS or an AP. This is the algorithm that the VHDC in Fig. 5 implements for the selection of the best route in response to the *relay* messages received from the candidate proxy nodes.

B. Route-Selection Algorithm to Optimize Battery Lifetime of System Including Ad Hoc Mode

For heterogeneous wireless networks, which include ad hoc networking, we aim to evenly balance over all the MNs the battery power consumed in relaying traffic for others. As presented

in Section III, in a heterogeneous wireless network without ad hoc support, the battery lifetime of each MN is considered to be related only to the RSS and the congestion (i.e., load) at its attachment point. However, in a heterogeneous wireless network supporting ad hoc mode, the amount of traffic that each MN relays has a great impact on the MN's battery lifetime, and hence, all MNs in the network must fairly participate in relaying each other's data frames. Thus, in this section, taking account of the amount of traffic load to be forwarded, we develop a route selection algorithm that maximizes, over the available routes, the remaining battery life of the "bottleneck" node, which has the lowest residual energy. This results in maximizing the overall battery lifetime of the system as well.

We consider a finite population of K MNs in a cellular coverage area as in Section III. Let D be the amount of traffic in bytes that has to be routed via some MNs in the cellular coverage area. For MN $u_j \in U$, which experiences a low downlink channel rate while receiving data frames from a BS of the cellular network or an AP, unless the VHDC can find an alternative point-to-point (one-hop) attachment point, a route will be selected by using ad hoc networking. Thus, the data from MN u_j are relayed over other MNs in the ad hoc network to reach an appropriate attachment point. Let p_j^b be the power consumption amount per byte of transmission at a given MN u_j. Then, the cost function is defined as

$$E_j = \frac{p_j}{p_j^b D}. \tag{18}$$

The maximum battery lifetime resulting from the selection of a given route r_s is determined by the minimum value of E_j over the path, i.e.,

$$L_s = \text{Min}_{\forall u_j \in r_s} E_j. \tag{19}$$

Let R be the set of all possible routes between MN u_j that is experiencing a degraded downlink channel rate and candidate attachment points via proxy MNs in the ad hoc network. We assume that the VHDC has already selected [using **Opt**-G in (17)] the optimal attachment point (AP or BS) with which the candidate proxy node is associated. Then, we select the route $r_{\max}$ with the maximum battery lifetime value from the set R as follows:

$$r_{\max} : \text{Max}_{\forall r_s \in R} L_s = \text{Max}_{\forall r_s \in R} \left(\text{Min}_{\forall u_j \in r_s} \frac{p_j}{p_j^b D} \right). \quad (20)$$

When the route discovery process is triggered for an MN u_j that is experiencing a low downlink channel rate, the battery lifetime information, i.e., E_j, is sent encapsulated in the header of a *route request* message as a *cost* field. When a relay node u_i $(i \neq j)$ receives the *route request* message, it calculates the value of E_i and compares it with the *cost* field in the received *route request*. If the calculated E_i is less than the value of the *cost* field, then E_i is copied into the *cost* field. This process is repeated until the *route request* message reaches a BS or an AP that has been selected by the VHDC using **Opt**-G. The sequence of signal flows corresponding to their operations is shown in Fig. 5.

V. PERFORMANCE EVALUATION

Equations (11), (14), and (17) in Section III are mixed integer programming (MIP) formulations for battery lifetime maximization and load balancing. These MIP problems can be solved using the well-known branch-and-bound algorithm [21]. First, we describe the simulation setup. Then, we present the simulation results detailing the total battery lifetime over all MNs and the load distribution across all APs and BSs.

A. Simulation Environment

We conducted simulations for a cellular coverage area that is covered by two overlapping BSs and five hotspots, as shown in Fig. 6(a). Furthermore, Fig. 6(b) shows our simulation topology for the case when a MANET/VANET is used as an enhancement to the cellular network and the hotspots. We simulated two test scenarios in which 50 and 100 MNs are dispersed, respectively, over the combined coverage area of the two BSs in the topology of Fig. 6(a). Within the cellular coverage area, each hotspot area is conceptually divided into three different concentric areas, as shown in Fig. 7. The innermost area RSS_1 has the strongest RSS, whereas the second area RSS_2, which is outside RSS_1, has a lower RSS than RSS_1. In addition, the third area RSS_3, which represents the remaining portion of the hotspot area, has the weakest RSS. As shown in Fig. 7, the RSS_2 region is potentially the horizontal handoff region, whereas RSS_3 is potentially the VHO area. It should be noted that, in realistic WLAN environments, RSS is highly variable over time, even at a fixed location, depending on several known/unknown parameters such as multipath fading, interference, and local movements. Instead, for each combination of MN and AP, to also factor in multipath fading and other physical layer effects, we select a randomized average
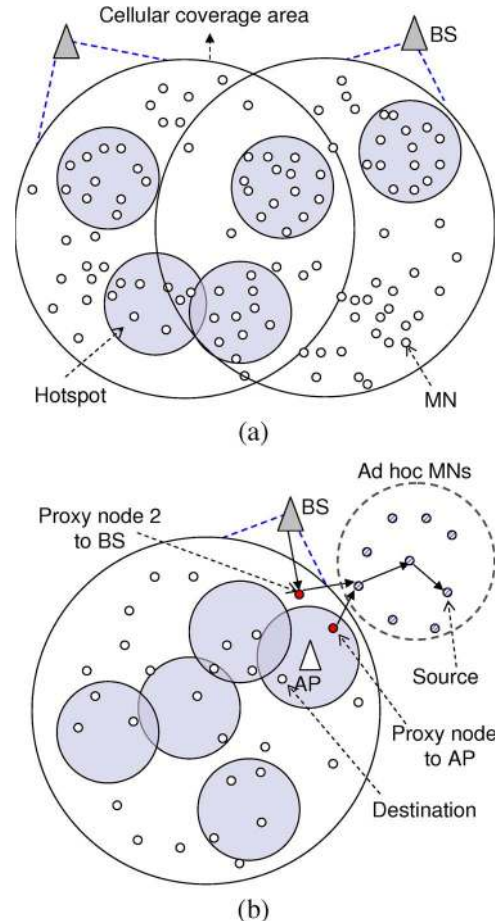

Fig. 6. Simulation topologies of heterogeneous wireless networks. (a) Two cases of 50 and 100 MNs for two BSs and five APs. (b) Network topology with ad hoc mode.
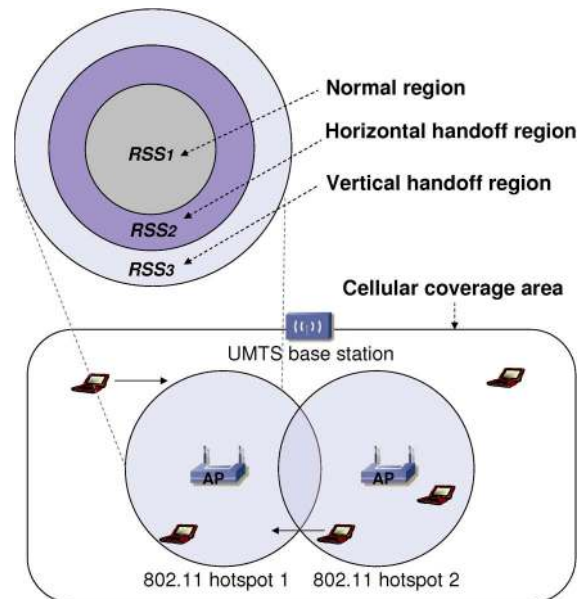

Fig. 7. Conceptual look at the RSS in a WLAN and example handoff regions in a heterogeneous network.

RSS value RSS_{ij}, where i and j denote the AP and the MN, respectively. This randomized average RSS value selection is done such that it broadly captures the effects of distance to the

AP (e.g., the concentric regions of Fig. 7) and the effects of the physical layer phenomena and time averaging.

At the beginning of the simulation run, MNs are evenly distributed over all WLAN areas, and hence, 10 MNs (first test case) or 20 MNs (second test case) are serviced by each of the five APs. The MNs move around during the entire simulation time. A random mobility model is used to characterize the movement of MNs inside a cellular coverage area. The RSS_{ij} values for all pairs of MN and AP association are reselected after each such movement, according to the method previously described. For simplicity, it is assumed in the simulations that each MN's RSS value is above the required threshold for making a connection to a BS if it is within the coverage area of that BS.

The requested data rate of MN j, which is denoted by r_j, can be one of the values from the set $\{64\text{ kb/s}, 128\text{ kb/s}, 192\text{ kb/s}\}$. When a new connection arrives, the associated data rate is uniformly selected from the three allowed data rates. The battery power of an MN j, which is denoted by p_j, is initialized at the onset of its connection to the value of 10^3 J. The rates of consumption of MN j's battery power in association with AP i and BS i are p_{ij} and $p_{ij}^{(c)}$, respectively. Each of these rates is assumed to be exponentially distributed with a mean of 5 mJ/s [24]. The bandwidth capacities of each AP and each BS B_i and $B_i^{(c)}$ are set to 20 and 2 Mb/s, respectively. We set the weights (or prices) associated with the AP and BS bandwidth usages w_a and w_c to values 1 and 10, respectively.

In our experiment, we used the TOMLAB[1] optimization package [22], and from the libraries thereof, CPLEX was used to solve the problem formulations described in Section III. We use the branch-and-bound algorithm in the CPLEX optimization package for solving the MIP optimization problems. We studied the battery lifetime and the evenness of load distribution for the two test cases. Ten independent simulation runs with a duration of 10 000 s each were performed, measurements were taken at intervals of 1000 s, and the results reported were averaged over the ten runs. Our two key performance metrics were measured over the simulation time considering all the MNs, APs, and BSs involved in the two test cases.

It is worth noting here that the computational complexity of the proposed optimization algorithm is very manageable. In addition, the computational complexity is limited due to the sparse nature of the $\mathcal{X}$ and $\mathbf{X}$ matrices [see (5) and (7)]. Majority of entries in these matrices are zero while performing the optimization computations; only the neighboring networks that have an RSS greater than a threshold are relevant from the perspective of MNs that require VHO. All experiments were run on an otherwise unloaded 2-GHz Pentium IV processor with 768 MB of memory. On average, the central processing unit (CPU) run time taken to solve the optimization was about 10 ms for both the 50- and 100-node topologies. It is to be noted that these CPU run times are small enough not to be of concern for the optimization computations for VHO network selection

in a realistic heterogeneous wireless network. In addition, these measurements were, in fact, obtained on a simple desktop computer, whereas the VHDC in real implementation would have the benefit of faster processors.

B. Simulation Results

In this section, we present and discuss simulation results for the topology of Fig. 6(a) and two test cases (50 and 100 MNs) described in Section V-A. To the best of our knowledge, there is no previous proposal that considered similar optimization objectives as we do (i.e., maximizing collective battery-life time and load balancing) for heterogeneous networks. Hence, we chose to compare the performance of our methods with that of a commonly known method, i.e., the strongest-signal first (SSF) method. The SSF method is basically a WLAN-first scheme (i.e., preferring an available WLAN over a cellular network), and in addition, when there is a choice of multiple APs, the AP with the strongest signal is selected. The comparisons are presented in terms of the overall system battery lifetime averaged over all MNs and the distributedness of load among the attachment points (i.e., APs and BSs).

As stated earlier, for a given set of loads and MNs' battery lifetimes, the values of α and β in solving the joint optimization problem in (16) and (17) can appropriately be selected to put different emphases on battery lifetime and load balancing. The values of weights α and β would typically be supplied by the network operator or carrier responsible for the maintenance of the network. For instance, the VHDCs for a region covering one or multiple APs and/or BSs can have algorithms that determine the values of the weights after obtaining the user profiles via the MIHF, as addressed in Section II, and then process them based on the network operator's policy [25]. For this study, based on some preliminary simulation runs with typical system and load parameters, we have determined that the first term in (16) (corresponding to battery lifetime) is typically about five orders of magnitude greater than the second term (corresponding to normalized load). This is naturally dependent on the measurement units used as well for each of the terms. Hence, for the joint optimization to meaningfully work, we must select β values to be in the ballpark of 10^5 times higher than those of α and vary each in its respective range to study performance sensitivity to their values.

The 95th-percentile confidence intervals for the measurement results (battery lifetime and load) reported here are within $\pm 1\%$ of the average based on ten simulation runs. Figs. 8 and 9 show the percentage remaining battery lifetime averaged over all MNs, at the end of the simulation run (i.e., at 10 000 s) for the two test cases (50 and 100 MNs, respectively) for various optimization methods. In these plots, 100% corresponds to the remaining battery lifetime at the beginning of the simulation. These methods include solving the battery lifetime optimization problem $\mathbf{Max}$-L, the load fairness optimization problem $\mathbf{Opt}$-F, and the joint optimization problem $\mathbf{Opt}$-G. For the joint optimization function, $\mathbf{Opt}$-G, α, and β are set such that $\beta/\alpha = 10^5$, 3×10^5, and 5×10^5, which are denoted as $\mathbf{Opt}$-$G1$, $\mathbf{Opt}$-$G2$, and $\mathbf{Opt}$-$G3$, respectively, in Figs. 8–13. As we would expect, $\mathbf{Max}$-L achieves the longest battery

---

[1]TOMLAB and CPLEX are commercially available software tools. This work makes use of them to generate illustrative simulation results, but NIST does not, in any way, recommend or favor their use over other similar or comparable products.
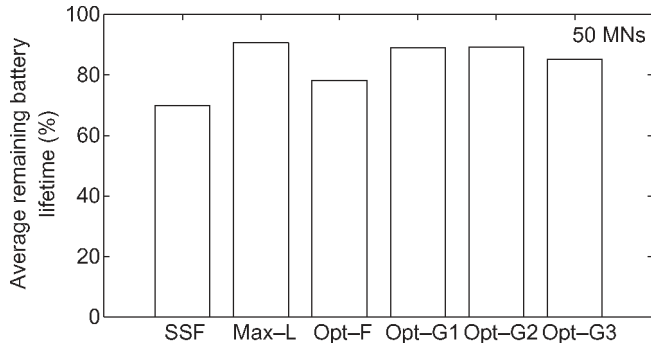
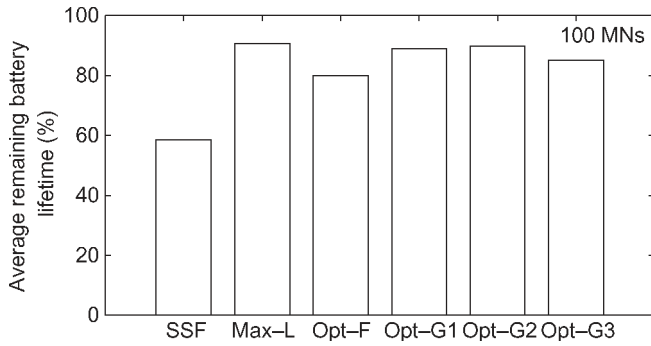Fig. 8. Average remaining battery lifetime for the test case with 50 MNs.

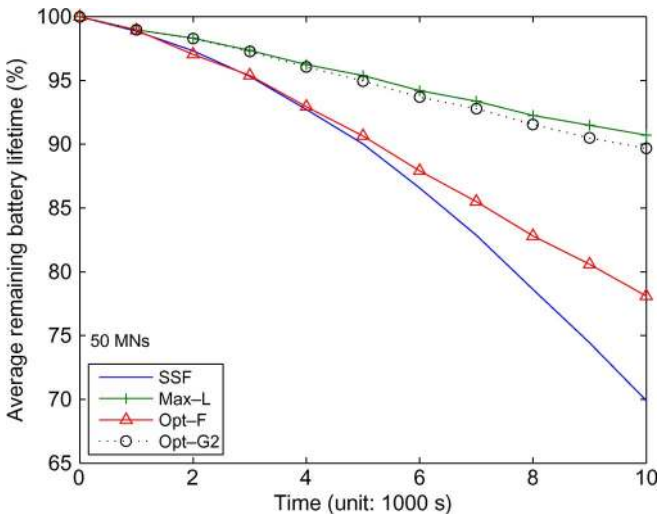Fig. 9. Average remaining battery lifetime for the test case with 100 MNs.

Fig. 10. Average remaining battery lifetime versus time when there are two BSs, five APs, and 50 MNs.
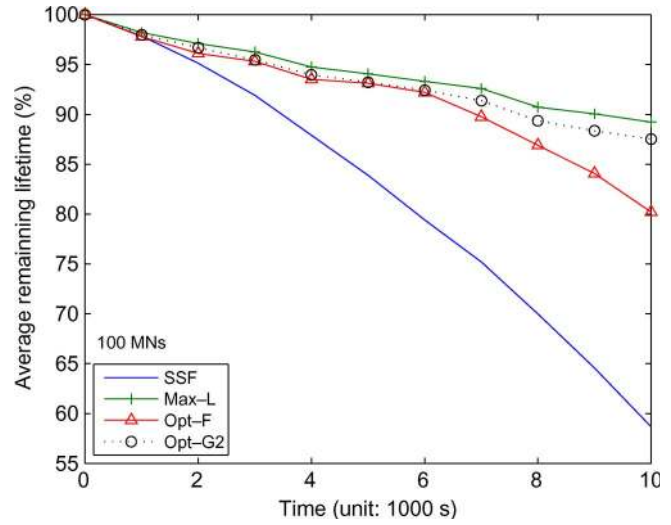

Fig. 11. Average remaining battery lifetime versus time when there are two BSs, five APs, and 100 MNs.

Fig. 12. Distributedness of load across attachment points when there are 50 MNs.
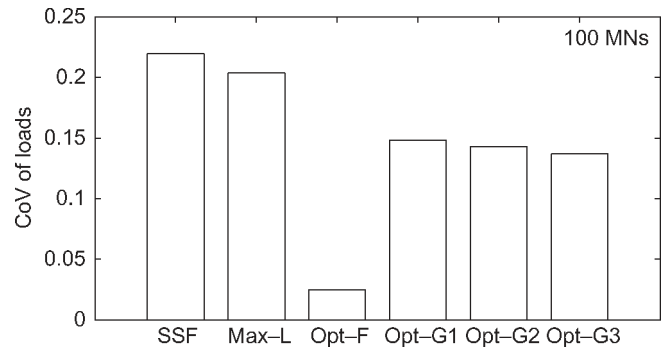
Fig. 13. Distributedness of load across attachment points when there are 100 MNs.

lifetime among all the cost functions or optimization methods in consideration (see Figs. 8 and 9). The SSF method connects the MNs to an available attachment point based on the strongest signal criterion only and, hence, performs worst in terms of battery life usage.

In Figs. 10 and 11, we plot the percentage remaining battery lifetime averaged over all MNs versus the simulation time for the two test cases of 50 and 100 MNs, respectively. We observe the same phenomenon as in Figs. 8 and 9. The battery lifetime for all the four schemes decreases with time. However, **Max**-*L* achieves the best performance in terms of average remaining battery lifetime, whereas SSF performs worst. In

Figs. 12 and 13, we plot the coefficient of variation of loads, which is defined as the standard deviation of loads observed at the APs divided by the mean load. This definition has extensively been used as a fairness metric in the literature for the illustration of the distributedness of load (i.e., load balancing) [23]. Figs. 12 and 13 show that **Opt**-*F* performs best among all the optimization methods, as expected, because **Opt**-*F* aims to evenly distribute the load among the attachment points accessible by MNs in a cellular coverage area. However, for the **Opt**-*F* method, the average battery lifetime is
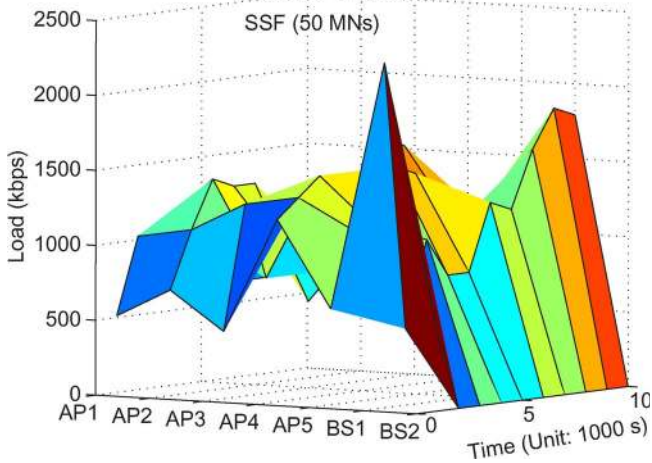
Fig. 14. Load status (in kilobits per second) at the APs and BSs versus the simulation time for the SSF method when there are 50 MNs.

Fig. 15. Load status (in kilobits per second) at the APs versus the simulation time for the **Max**-L method when there are 50 MNs.

Fig. 16. Load status (in kilobits per second) at the APs and BSs versus the simulation time for the **Opt**-F method when there are 50 MNs.

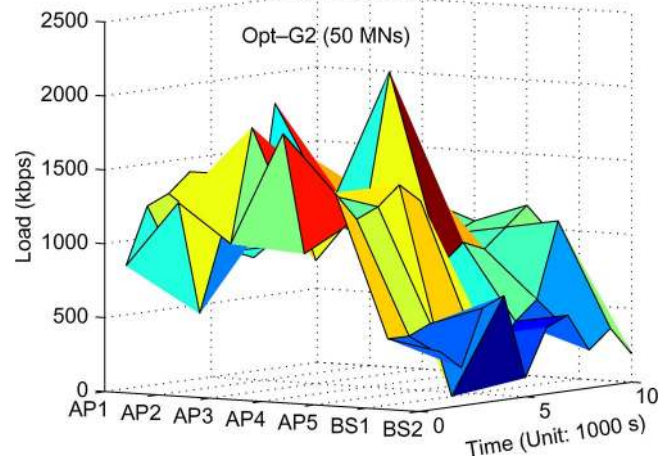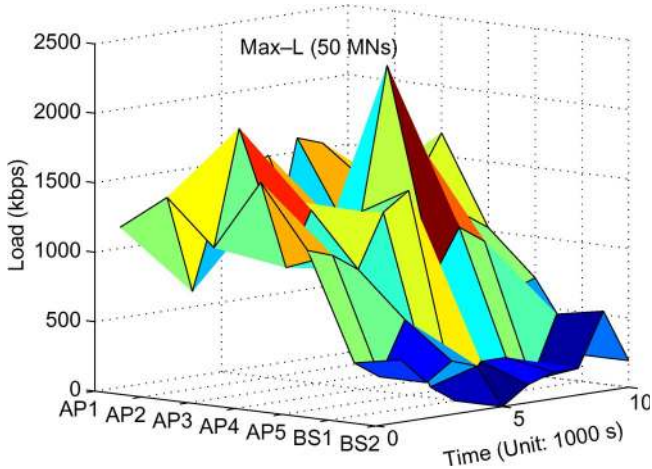shorter compared with those for **Max**-L, **Opt**-$G1$, **Opt**-$G2$, and **Opt**-$G3$, as was noted in Figs. 8 and 9. SSF achieves the worst performance in terms of the distributedness of load and the battery lifetime. The weighted combined optimization

Fig. 17. Load status (in kilobits per second) at the APs and BSs versus the simulation time for the **Opt**-$G2$ method when there are 50 MNs.

Fig. 18. Load status (in kilobits per second) at the APs and BSs versus the simulation time for the SSF method when there are 100 MNs.

method **Opt**-G provides performance that lies in between those for **Max**-L and **Opt**-F in terms of either of the two performance metrics, i.e., the battery lifetime or load fairness. In Figs. 14–17, we plot the overall load at each AP and each BS versus the simulation time for the first test case with 50 MNs active in the test coverage area. Similarly, the overall loads for the second test case with 100 active MNs are plotted in Figs. 18–21. These figures show how the load is distributed among the APs and BSs by the proposed cost functions and the SSF approach during the entire simulation time. The detailed load distribution data corresponding to these figures are given in Tables II–VII. As mentioned in Section III, it is known that the bandwidth price level for WLANs is cheaper than that for cellular networks. Thus, in our simulation tests, w_c is relatively larger than w_a, so that the APs are selected in preference to the BSs when an attachment point needs to be selected. That is, we aim to use a cheaper WLAN bandwidth (particularly, for multimedia traffic) in preference to the BS bandwidth. Through our proposed joint optimization method, the VHDC has the flexibility to manipulate the relative emphasis on extending battery lifetime versus load balancing. We observe from Fig. 14 that, under the SSF scheme, one of the five

Fig. 19. Load status (in kilobits per second) at the APs and BSs versus the simulation time for the **Max**-*L* method when there are 100 MNs.
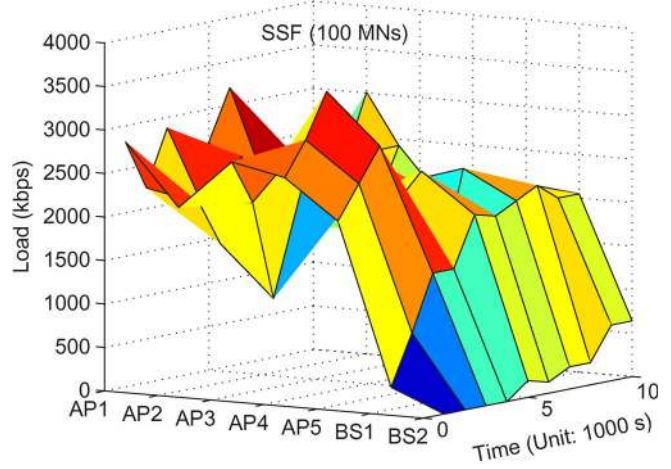

Fig. 20. Load status (in kilobits per second) at the APs and BSs versus the simulation time for the **Opt**-*F* method when there are 100 MNs.
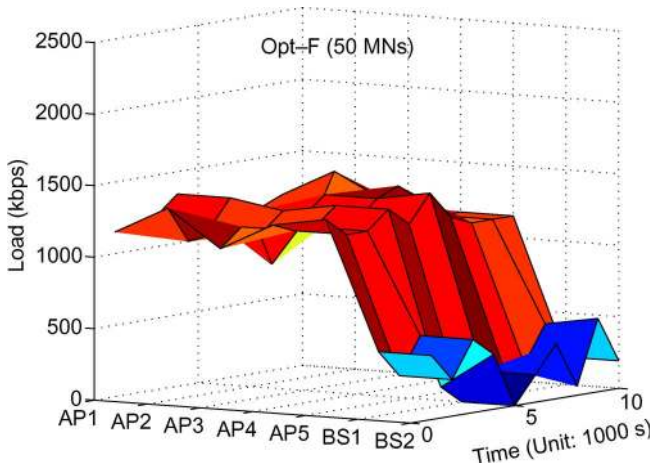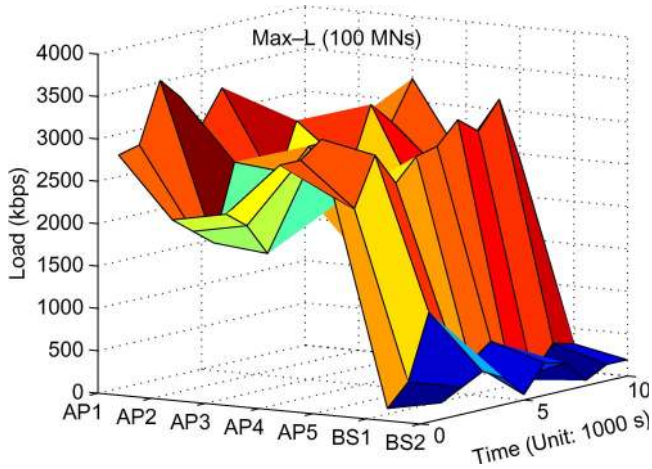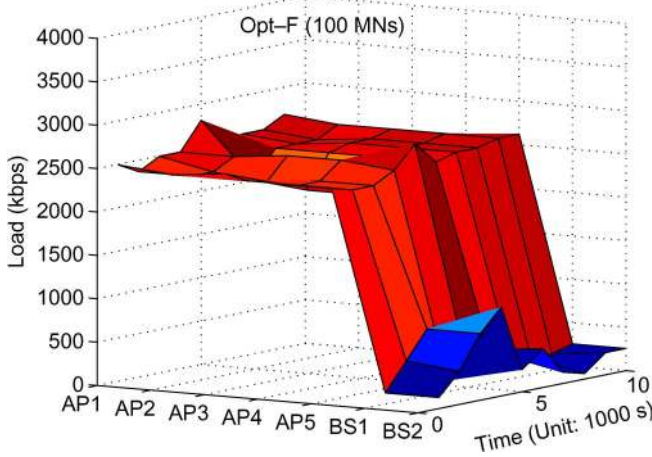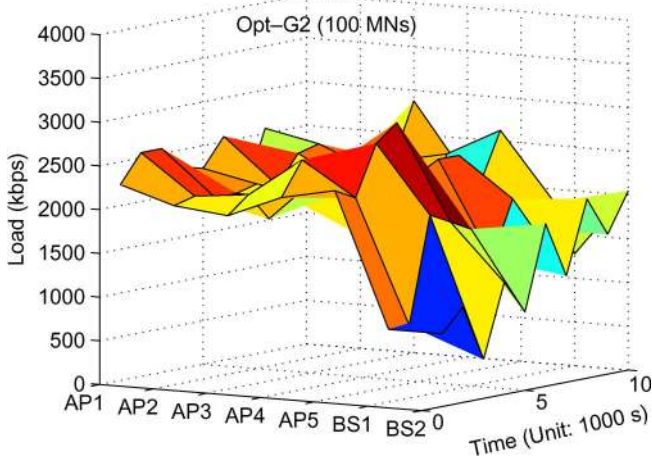

Fig. 21. Load status (in kilobits per second) at the APs and BSs versus the simulation time for the **Opt**-*G*2 method when there are 100 MNs.

APs (AP4 in the graph) carries the maximum load of 1664 kb/s at a simulation unit time of 6000 s, and the maximum load of 2304 kb/s is associated with one BS (BS1) at the time of 1000 s. We observe that the SSF method does a poor job of not only distributing the load very unevenly across APs but

also favoring BS1 at the expense of BS2 in the simulation test case with 50 MNs. For the **Opt**-*F* method, the load is quite evenly distributed over the APs mostly within an approximate narrow range of 1088–1408 kb/s, as shown in Fig. 16. The data corresponding to Fig. 16 are shown in Table II. Similar observations can be made for the test case with 100 MNs from the plots shown in Figs. 18 and 20. Based on the two sets of plots shown in Figs. 12–19, the following two other important observations can be made about the advantages of our proposed methods **Max**-*L*, **Opt**-*F*, and Max $G(\mathbf{X}, \alpha, \beta)$ over the SSF method: 1) These methods show a lower preference for BSs over APs, which is desirable since APs are better suited to carry higher bandwidth multimedia calls. 2) Parameters α and β can suitably be tuned by the network operator to achieve pure load-balancing optimization, pure battery lifetime optimization, or a suitable weighted combination of the two.

C. Battery Lifetime Results for Heterogeneous Networks Including Ad Hoc Mode

In this section, we compare the performance of the proposed route-selection algorithm described in Section IV with that of DSR. The results presented here are obtained from the simulation model described in Section V-A [see Fig. 6(b)], wherein the number of MNs in an ad hoc area is set to 40. As shown in Fig. 6(b), the MNs operating in ad hoc mode are not within the coverage of any AP or BS but are in range of each other via their short-range radios. This figure also shows two example routes from a source node (i.e., ad hoc-mode MN) to two candidate proxy nodes; proxy node 1 reaches the destination via an AP, and proxy node 2 does the same via a BS. The route-selection algorithm $r_{\max}$ proposed in Section IV may typically select a different route from that selected by the DSR algorithm, because our $r_{\max}$ algorithm is enhanced to take into account the battery lifetimes of the MNs in the route.

In our simulation runs, a pair of nodes consisting of one each in the ad hoc and cellular coverage areas is randomly selected as the source and destination nodes, respectively. Five such pairs of nodes are selected per 1000 s of time, and one connection is generated each time. All the MNs are randomly distributed and randomly move. When they move, a new route is selected between the pair of nodes if the current route becomes unusable due to the movement and power considerations. The amount of data sent per connection from the source node is exponentially distributed with mean D kB per connection. D is set to one of these three values: 5, 10, and 15 kB. The initial battery power of each MN is 1000 mJ. We use the power consumption model developed in [24] for the WLAN interface, where the energy consumed by a network interface as it sends and receives point-to-point messages is described as 0.8 mJ $+ 2.4$ mJ/kB $\times D$. Ten independent simulation runs with a duration of 20 000 s each are performed, measurements are taken at intervals of 1000 s, and the results reported are averaged over the ten runs.

Here, our focus is on the power consumed by proxy nodes while forwarding packets on behalf of other nodes in the ad hoc area. The proposed algorithm $r_{\max}$ aims to improve the longevity of the network by making the battery life for proxy MNs last longer. Accordingly, in this algorithm, the load gets

TABLE II
FOR SSF AND **Max**-L, LOAD STATUS (IN KILOBITS PER SECOND) AT THE APs AND BSs DURING SIMULATION
WHEN THERE ARE TWO BSs, FIVE APs, AND 50 MNs (TIME UNIT: 1000 s)

Time	SSF (50-node)							**Max**-L (50-node)						
	AP1	AP2	AP3	AP4	AP5	BS1	BS2	AP1	AP2	AP3	AP4	AP5	BS1	BS2
1	512	704	448	1216	640	2304	512	1152	1408	1088	1600	1152	384	448
2	1024	1088	1280	1344	1152	512	0	1216	704	1920	960	1088	256	256
3	1088	1408	768	1472	1152	1088	0	1280	1088	1344	1344	960	640	384
4	704	1344	896	832	1536	832	0	1408	1472	1344	1088	1344	128	320
5	1024	1344	576	1024	1472	832	0	1088	1600	832	1280	1472	0	0
6	768	704	832	1664	1152	1280	0	832	896	1088	2304	832	256	128
7	640	896	1024	1600	1088	1216	0	768	1088	1216	1792	1152	256	192
8	640	960	1088	896	1152	1600	0	1600	1024	1088	1024	1024	64	192
9	768	1024	1152	1024	768	1856	0	1536	1280	1344	1152	640	512	576
10	896	896	640	1024	384	1792	0	1216	1216	1664	1024	704	192	192

TABLE III
FOR **Opt**-F AND **Opt**-$G1$, LOAD STATUS (IN KILOBITS PER SECOND) AT THE APs AND BSs DURING SIMULATION
WHEN THERE ARE TWO BSs, FIVE APs, AND 50 MNs (TIME UNIT: 1000 s)

Time	**Opt**-F (50-node)							**Opt**-$G1$ (50-node)						
	AP1	AP2	AP3	AP4	AP5	BS1	BS2	AP1	AP2	AP3	AP4	AP5	BS1	BS2
1	1152	1344	1088	1280	1344	448	448	832	1344	1024	1728	1408	448	384
2	1152	1088	1216	1216	1216	256	256	1216	512	1792	960	1216	448	256
3	1216	1152	1152	1216	1216	512	512	1280	1024	1216	1344	1280	512	640
4	1344	1344	1280	1344	1344	128	384	1408	1408	1280	1088	1408	0	704
5	1216	1216	1216	1216	1216	0	0	1088	1472	832	1280	1280	192	0
6	1088	832	1344	1344	1408	192	192	704	896	1280	2112	832	64	512
7	1152	1216	1216	1408	1216	192	384	768	1088	1216	1536	1152	256	704
8	1152	1088	1152	1088	1152	192	64	1792	1024	1088	896	1088	384	256
9	1216	1408	1216	1152	1152	448	512	1664	1280	1152	960	640	896	384
10	1088	1088	1152	1152	1152	192	192	1152	1216	1344	1024	832	576	192

TABLE IV
FOR **Opt**-$G2$ AND **Opt**-$G3$, LOAD STATUS (IN KILOBITS PER SECOND) AT THE APs AND BSs DURING SIMULATION
WHEN THERE ARE TWO BSs, FIVE APs, AND 50 MNs (TIME UNIT: 1000 s)

Time	**Opt**-$G2$ (50-node)							**Opt**-$G3$ (50-node)						
	AP1	AP2	AP3	AP4	AP5	BS1	BS2	AP1	AP2	AP3	AP4	AP5	BS1	BS2
1	832	1280	1024	1792	1408	448	384	832	1088	1152	1472	1472	832	832
2	1216	512	1792	960	1216	448	256	1216	512	1792	960	1088	576	256
3	1280	1024	1216	1344	1280	512	640	1280	1216	1216	1152	1280	576	640
4	1408	1408	1280	1088	1408	0	704	1408	1408	1280	1088	1408	0	704
5	896	1344	832	1280	1280	384	128	896	1344	832	1280	1280	384	128
6	832	896	1280	2112	832	256	448	832	896	1664	1728	832	256	448
7	768	1088	1280	1472	960	448	512	768	1024	1344	1472	960	512	512
8	1792	1152	1024	896	896	576	256	1792	1280	960	896	896	640	256
9	1472	1088	960	960	1024	1088	384	1472	960	960	960	832	1408	384
10	1088	1152	1152	1024	1152	768	192	1088	1152	1024	1152	1152	1088	192

TABLE V
FOR SSF AND **Max**-L, LOAD STATUS (IN KILOBITS PER SECOND) AT THE APs AND BSs DURING SIMULATION
WHEN THERE ARE TWO BSs, FIVE APs, AND 100 MNs (TIME UNIT: 1000 s)

Time	SSF (100-node)							**Max**-L (100-node)						
	AP1	AP2	AP3	AP4	AP5	BS1	BS2	AP1	AP2	AP3	AP4	AP5	BS1	BS2
1	2816	2112	2688	2560	2112	256	0	2752	2048	2176	2816	2496	64	192
2	2240	2112	2176	2944	2496	832	0	2816	1856	1984	2816	2304	320	320
3	2880	1600	1024	3456	2880	1472	0	3520	1664	1600	3008	2880	1088	448
4	2240	2560	1792	2112	2240	1472	0	3264	2560	2496	2240	2496	704	320
5	2624	1344	1920	1792	2496	2048	192	2880	1856	2752	1472	2752	384	64
6	3200	1600	2752	1344	1408	1984	128	3264	2176	2752	1344	2816	576	384
7	2240	2304	1920	2240	2432	2112	256	2304	2880	2368	2048	3072	64	320
8	2240	2176	1920	2176	1856	2240	256	2304	2624	3072	1856	2880	64	64
9	1664	2304	2496	1792	2176	2048	640	2304	2624	2816	2240	3200	384	192
10	1216	3008	2048	1408	2112	2048	640	1856	2560	3264	2304	2432	320	192

balanced over all accessible proxy nodes, so that the MNs in the ad hoc area would be able to sustain connectivity for a longer period with the MNs outside the ad hoc area. The performance of our proposed $r_{\max}$ algorithm and that of DSR are compared in Table VIII. The 95th-percentile confidence intervals for the measurements reported in this table are within $\pm 1\%$ of the average based on ten independent simulation runs. This table compares the two algorithms using two separate metrics: 1) the

TABLE VI
FOR **Opt-**F AND **Opt-**$G1$, LOAD STATUS (IN KILOBITS PER SECOND) AT THE APs AND BSs DURING SIMULATION
WHEN THERE ARE TWO BSs, FIVE APs, AND 50 MNs (TIME UNIT: 1000 s)

Time	**Opt-**F (100-node)							**Opt-**$G1$ (100-node)						
	AP1	AP2	AP3	AP4	AP5	BS1	BS2	AP1	AP2	AP3	AP4	AP5	BS1	BS2
1	2496	2432	2496	2432	2432	128	128	2496	2048	1984	2496	2496	576	448
2	2368	2368	2368	2368	2368	448	384	2560	2112	2176	2688	2304	576	768
3	2496	2368	2304	2368	2368	768	768	2688	2048	1664	2624	2688	2048	448
4	2496	2496	2560	2560	2496	128	1024	2432	2560	2240	2048	2752	1920	832
5	2816	2176	2112	2112	2752	192	256	2496	2240	2432	1664	2368	896	576
6	2496	2496	2496	2496	2496	384	448	2816	2112	2432	1792	2624	704	1216
7	2560	2496	2560	2560	2560	256	128	2048	2624	1984	2496	2688	960	768
8	2560	2496	2560	2560	2560	192	64	2240	2496	2432	1792	2432	960	1216
9	2688	2624	2624	2624	2624	192	256	2304	1920	2560	2688	2688	1280	704
10	2368	2496	2304	2368	2624	256	256	1856	2176	3072	2304	2240	704	1216

TABLE VII
FOR **Opt-**$G2$ AND **Opt-**$G3$, LOAD STATUS (IN KILOBITS PER SECOND) AT THE APs AND BSs DURING SIMULATION
WHEN THERE ARE TWO BSs, FIVE APs, AND 50 MNs (TIME UNIT: 1000 s)

Time	**Opt-**$G2$ (100-node)							**Opt-**$G3$ (100-node)						
	AP1	AP2	AP3	AP4	AP5	BS1	BS2	AP1	AP2	AP3	AP4	AP5	BS1	BS2
1	2240	2048	1984	2240	2368	832	832	2048	1856	1984	2240	2176	1216	1024
2	2560	2112	2176	2624	2240	832	1088	2432	2304	2176	2624	2240	1024	1280
3	2560	2048	1856	2432	2816	2048	448	2304	2176	2176	2176	2816	2048	448
4	2304	2048	2048	2176	3008	1920	1280	2048	2048	1856	2112	2688	1856	2048
5	2240	2112	2048	1600	2368	1792	896	1984	2112	2048	1856	2240	1984	1536
6	2560	2048	2240	1600	2496	1408	1856	2368	1984	2368	1600	2496	1536	2048
7	1856	2368	2048	2112	2496	2048	1216	1792	2176	2176	2304	2496	2048	1344
8	2560	2432	2176	1472	2112	1664	2048	2560	2240	1984	1856	2112	1664	2048
9	2112	1984	2240	2368	2688	1920	1600	1856	2048	2240	2368	2688	2043	1536
10	1792	1984	2880	2048	1984	1280	2048	2240	2048	2624	1856	1984	1344	2048

TABLE VIII
(a) REMAINING ENERGY (IN MILLIJOULES) OF EACH PROXY NODE AFTER
20 000 s OF SIMULATION TIME. (b) AVERAGE CVE FOR THE PROXY NODES
MEASURED AT 1000-s INTERVALS AND AVERAGED OVER THE
SIMULATION TIME. (THE 95th-PERCENTILE CONFIDENCE INTERVALS FOR
THE MEASUREMENTS REPORTED IN THIS TABLE ARE WITHIN ±1% OF
THE AVERAGE BASED ON TEN SIMULATION RUNS.)

(a)

	$D = 5$		
	Proxy 1	Proxy 2	Proxy 3
DSR	743.3	1000	1000
r_{max}	913.8	910.3	919.3
	$D = 10$		
	Proxy 1	Proxy 2	Proxy 3
DSR	456.8	1000	1000
r_{max}	812.4	806.4	838
	$D = 15$		
	Proxy 1	Proxy 2	Proxy 3
DSR	254	1000	1000
r_{max}	702.6	783.5	768

(b)

D	5	10	15
DSR	0.08	0.18	0.27
r_{max}	0.018	0.043	0.077
$\frac{\text{CVE of DSR}}{\text{CVE of } r_{max}}$	4.44	4.19	3.51

Fig. 22. CVE for the remaining energy of the three proxy nodes in the heterogeneous network including the ad hoc mode.

remaining energy of each of the three available proxy nodes at the end of simulation run length of 20 000 s and 2) the covariance of the remaining energy CVE for the three proxy nodes (measured at intervals of 1000 s and averaged over the simulation run). It is evident that the r_{max} algorithm consistently performs better than the DSR. As an example, in Table VIII(a), we see that, for the case of $D = 15$ kB, the remaining energy
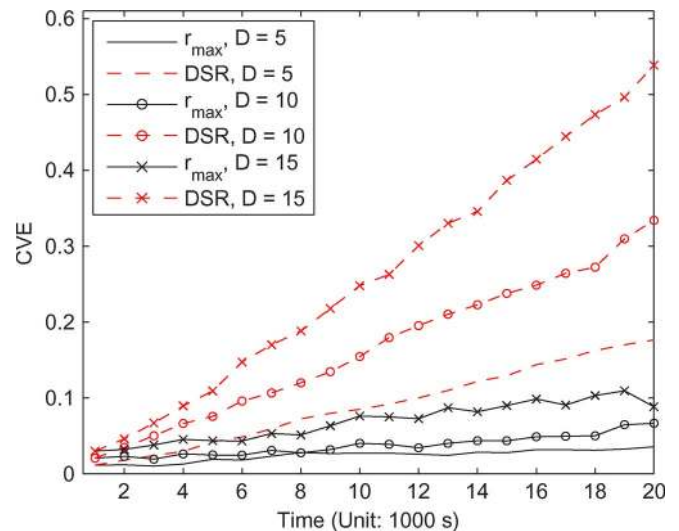
of Proxy 1 is 254 and 702.6 mJ, respectively, for the DSR and r_{max} algorithms. This effectively means that the probability that Proxy 1 MN will turn off is much higher for DSR as compared with that for the r_{max} algorithm. In essence, the proposed r_{max} algorithm evenly distributes the load across the three proxy MNs so that each has about equal remaining energy. This is further illustrated in Table VIII(b) and Fig. 22 by comparing the CVE values for the DSR and r_{max} algorithms. The improvement in the CVE values for the r_{max} algorithm over DSR is quite significant and is lower by factors of 4.44, 4.19, and 3.51 for the cases of $D = 5$, 10, and 15 kB, respectively.

VI. Conclusion

When connections need to migrate between heterogeneous networks for performance and high-availability reasons, then seamless VHO is a necessary first step. In the near future, vehicular and other mobile applications will expect seamless VHO between heterogeneous access networks, which will include WLANs, cellular networks (UMTS, CDMA2000), WiMAX, and VANETs/MANETs.

New metrics for VHO continue to emerge, and the use of new metrics makes the VHD process increasingly more complex. In this paper, we have tried to highlight the metrics best suited for the VHDs. We have also proposed a generalized VHD algorithm that seeks to optimize a combined cost function involving the battery lifetime of the MNs and load balancing over the APs/BSs. We have further proposed an enhanced algorithm for the case when ad hoc-mode MNs that form VANETs/MANETs are included in the heterogeneous networks. This latter algorithm allows the proxy nodes, which provide connectivity to the nearest AP or BS for the ad hoc-mode MNs, to share transit loads, with the goal of balancing their consumption of battery power. Our performance results based on detailed simulations illustrate that the proposed algorithms perform much better than the conventional optimization based on the SSF method, which is based on RSS alone. Our proposed method gives the network operator the leverage to easily vary the emphasis from maximizing the overall system battery lifetime for MNs to seeking fairness of load distribution over APs and BSs, with weighted combinations in between.

Appendix

To take into account the fairness of load distribution, a simple but useful lemma is provided as follows:

Lemma 1: Let $\{b_i\}_{i=1}^I$ be a finite sequence of real numbers and $A = (1/I) \sum_{i=1}^I b_i$ be the mean value of the sequence. Then

$$\sum_{i=1}^I b_i^2 = \sum_{i=1}^I (b_i - A)^2 + IA^2. \tag{21}$$

Proof: Since $\sum_{i=1}^I (b_i - A) = 0$

$$\sum_{i=1}^I b_i^2 = \sum_{i=1}^I [(b_i - A) + A]^2$$

$$= \sum_{i=1}^I \left[(b_i - A)^2 + 2A(b_i - A) + A^2 \right]$$

$$= \sum_{i=1}^I (b_i - A)^2 + 2A \sum_{i=1}^I (b_i - A) + \sum_{i=1}^I A^2$$

$$= \sum_{i=1}^I (b_i - A)^2 + IA^2. \tag{22}$$

References

[1] *3GPP System to WLAN Interworking: System Description (Release 7)*. (2006, Mar.). 3GPP TR 23.234 v7.1.0. [Online]. Available: http://www.3gpp.org/specs/specs.htm

[2] A. K. Salkintzis, "Interworking techniques and architectures for WLAN/3G integration toward 4G mobile data networks," *IEEE Wireless Commun.*, vol. 11, no. 3, pp. 50–61, Jun. 2004.

[3] M. Buddhikot, G. Chandranmenon, S. Han, Y. W. Lee, S. Miller, and L. Salgarellim, "Integration of 802.11 and third-generation wireless data networks," in *Proc. IEEE INFOCOM*, San Francisco, CA, Mar. 2003, vol. 1, pp. 503–512.

[4] V. Varma, S. Ramesh, K. Wong, and J. Friedhoffer, "Mobility management in integrated UMTS/WLAN networks," in *Proc. IEEE ICC*, Ottawa, ON, Canada, May 2003, vol. 2, pp. 1048–1053.

[5] T. B. Zahariadis, "Migration toward 4G wireless communications," *IEEE Wireless Commun.*, vol. 11, no. 3, pp. 6–7, Jun. 2004.

[6] J. McNair and F. Zhu, "Vertical handoffs in fourth-generation multinetwork environments," *IEEE Wireless Commun.*, vol. 11, no. 3, pp. 8–15, Jun. 2004.

[7] C. Guo, Z. Guo, Q. Zhang, and W. Zhu, "A seamless and proactive end-to-end mobility solution for roaming across heterogeneous wireless networks," *IEEE J. Sel. Areas Commun.*, vol. 22, no. 5, pp. 834–848, Jun. 2004.

[8] R. Chakravorty, P. Vidales, K. Subramanian, I. Pratt, and J. Crowcroft, "Performance issues with vertical handovers—Experiences from GPRS cellular and WLAN hot-spots integration," in *Proc. IEEE PerCom*, Orlando, FL, Mar. 2004, pp. 155–164.

[9] N. Nasser, A. Hasswa, and H. Hassanein, "Handoffs in fourth generation heterogeneous networks," *IEEE Commun. Mag.*, vol. 44, no. 10, pp. 96–103, Oct. 2006.

[10] *Standard and Metropolitan Area Networks: Media Independent Handover Services*, IEEE Std. 802-21, Jan. 2006.

[11] H. Wu, C. Qiao, S. De, and O. Tonguz, "Integrated cellular and ad hoc relaying systems: iCAR," *IEEE J. Sel. Areas Commun.*, vol. 19, no. 10, pp. 2105–2115, Oct. 2001.

[12] D. Cavalcanti, D. Agrawal, C. Corderio, B. Xie, and A. Kumar, "Issues in integrating cellular networks WLANs, and MANETs: A futuristic heterogeneous wireless network," *IEEE Wireless Commun.*, vol. 12, no. 3, pp. 30–41, Jun. 2005.

[13] A. Dutta, S. Das, D. Famolari, Y. Ohba, K. Taniuchi, T. Kodama, and H. Schulzrinne, "Seamless handoff across heterogeneous networks—An 802.21 centric approach," in *Proc. IEEE WPMC*, Aalborg, Denmark, Sep. 2005.

[14] *NIST Seamless and Secure Mobility Project*. [Online]. Available: http://www.antd.nist.gov/seamlessandsecure.shtml#project

[15] S. J. Yoo, D. Cypher, and N. Golmie, "LMS predictive link triggering for seamless handovers in heterogeneous wireless networks," in *Proc. MILCOM*, Orlando, FL, Oct. 28–30, 2007, pp. 1–7.

[16] G. Lampropoulos, A. K. Salkintzis, and N. Passas, "Media-independent handover for seamless service provision in heterogeneous networks," *IEEE Commun. Mag.*, vol. 46, no. 1, pp. 64–71, Jan. 2008.

[17] H. Zhai, J. Wang, and Y. Fang, "Providing statistical QoS guarantee for voice over IP in the IEEE 802.11 Wireless LANs," *IEEE Wireless Commun.*, vol. 13, no. 1, pp. 36–43, Feb. 2006.

[18] H. Zhai, X. Chen, and Y. Fang, "A call admission and rate control scheme for multimedia support over IEEE 802.11 Wireless LANs," *Wireless Netw.*, vol. 12, no. 4, pp. 451–463, Jul. 2006.

[19] D. Johnson, D. Maltz, and Y. Hu, *The dynamic source routing protocol for mobile Ad Hoc Networks (DSR)*, Jul. 2004. Internet Draft, draft-ietf-manet-dsr-10.txt.

[20] H. Luo, R. Ramjee, P. Sinha, L. Li, and S. Lu, "UCAN: A unified cellular and Ad-Hoc network architecture," in *Proc. ACM Mobicom*, San Diego, CA, Sep. 2003, pp. 353–367.

[21] R. Fletcher and S. Leyffer, "Numerical experience with lower bounds for MIQP branch-and-bound," *SIAM J. Optim.*, vol. 8, no. 2, pp. 604–616, 1998.

[22] *TOMLAB: A General Purpose MATLAB Environment for Optimization*. [Online]. Available: http://tomlab.biz.com

[23] R. Jain, *The Art of Computer Systems Performance Analysis: Techniques for Experimental Design, Measurement, Simulation, and Modeling.* New York: Wiley-Interscience, Apr. 1991.

[24] L. Feeney and M. Nilsson, "Investigating the energy consumption of a wireless network interface in an ad hoc networking environment," in *Proc. IEEE INFOCOM*, Anchorage, AK, 2001, vol. 3, pp. 1548–1557.

[25] K. P. Demestichas, A. Koutsorodi, E. Adamopoulou, and M. Theologou, "Modelling user preferences and configuring services in B3G devices," *Wireless Netw.*, vol. 14, no. 5, pp. 699–713, Oct. 2008.

SuKyoung Lee (M'04) received the B.S., M.S., and Ph.D. degrees in computer science from Yonsei University, Seoul, Korea, in 1992, 1995, and 2000, respectively.

From 2000 to 2003, she was with the Advanced Networking Technologies Division, National Institute of Standards and Technology, Gaithersburg, MD. She is currently an Assistant Professor with the Department of Computer Science, Yonsei University. Her current research interests include wireless and mobile networks and optical data networking.

Kotikalapudi Sriram (S'80–M'82–SM'97–F'00) received the B.S. and M.S. degrees from the Indian Institute of Technology, Kanpur, India, and the Ph.D. degree from Syracuse University, Syracuse, NY, all in electrical engineering.

He is currently a Senior Researcher with the Advanced Networking Technologies Division, National Institute of Standards and Technology, Gaithersburg, MD. From 1983 to 2001, he was with Bell Laboratories (the innovations arm of Lucent Technologies and formerly that of AT&T), where he has been a Consulting Member of Technical Staff (approximately top 1% of engineers in 2001) and a Distinguished Member of Technical Staff. He is a contributing author and a Coeditor of *Cable Modems: Current Technologies and Applications* (Piscataway, NJ: IEEE Press, 1999). He is a coinventor on a patent related to quality-of-service management for voice-over-IP (VOIP) that was recognized by the *MIT Technology Review Magazine* as one of the five Killer Patents in 2004. He has authored more than 60 papers in various IEEE journals and other international journals and major conference proceedings. He is the holder of 17 U.S. patents. His research interests include performance modeling, network architecture, Internet routing protocol security and scalability, design of protocols and algorithms for multiservice broadband networks, VOIP, wireless access networks, IP/MPLS/ATM traffic controls, and hybrid fiber-coax networks.

Kyungsoo Kim received the B.S., M.S., and Ph.D. degrees in mathematics from the Korea Advanced Institute of Science and Technology, Daejeon, Korea, in 1996, 1998, and 2003, respectively.

From 2003 to 2006, he was a Postdoctoral Researcher with the Impedance Imaging Research Center, Kyung Hee University, Seoul, Korea; the BK21 Mathematical Sciences Division, Seoul National University; and the National Institute of Mathematical Science, Seoul, Korea. He is currently an Assistant Professor with the Department of Mathematics, Kyonggi University, Suwon, Korea. His current research interests include network optimization and vehicular computing systems, numerical analysis, optimization, and mathematical modeling.

Yoon Hyuk Kim received the B.S., M.S., and Ph.D. degrees in mechanical engineering from the Korea Advanced Institute of Science and Technology, Daejeon, Korea, in 1992, 1994, and 2000, respectively.

From 2000 to 2002, he was with the Orthopaedic Biomechanics Laboratory, Johns Hopkins University, Baltimore, MD. He is currently an Assistant Professor with the Department of Mechanical Engineering, Kyung Hee University, Yongin, Korea. His current research interests include network optimization and vehicular computing systems and biomechanical and biomedical engineering.

Nada Golmie (A'97–M'03) received the Ph.D. degree in computer science from the University of Maryland, College Park.

Since 1993, she has been a Research Engineer and the Manager of the High-Speed Network Technologies Group with the Advanced Networking Technologies Division, National Institute of Standards and Technology, Gaithersburg, MD. She is the author of *Coexistence in Wireless Networks: Challenges and System-Level Solutions in the Unlicensed Bands* (Cambridge Univ. Press, 2006). She has also authored more than 100 papers in professional conference proceedings and journals. She has contributed to international standard organizations and industry-led consortia. Her research interests include media access control and protocols for wireless networks.